Thin-Walled Structures 117 (2017) 356–366

Contents lists available at ScienceDirect

Thin-Walled Structures

journal homepage: www.elsevier.com/locate/tws

Model reduction in thin-walled open-section composite beams using variational asymptotic method. Part I: Theory☆

Dineshkumar Harursampath[a], Ajay B. Harish[b,*], Dewey H. Hodges[c]

[a] Department of Aerospace Engineering, Indian Institute of Science, Bangalore 560012, India
[b] Institute of Continuum Mechanics, Leibniz Universität Hannover, Appelstr. 11, Hannover 30167, Germany
[c] Daniel Guggenheim School of Aerospace Engineering, Georgia Institute of Technology, Atlanta, GA 30332, USA

ARTICLE INFO

Keywords:
Anisotropic
Asymptotic
Beam
Bending
Cantilever
Composite materials
Fibre reinforced
Laminated
Stochastic
Warping
Thin-walled
Open-section
Variational Asymptotic Method
Trapeze effect
Vlasov effect
Model reduction

ABSTRACT

This two-part work describes the development of a comprehensive and reliable tool for analysis of the most commonly used geometries of thin-walled, open-section composite beams. Part one describes formulation of an asymptotically-correct reduced order model and simple validation examples. The model, developed using the mathematically rigorous Variational Asymptotic Method (VAM), is capable of capturing all nonlinear and non-classical effects observed in anisotropic beams. It leads to closed forms solutions and thus rapid, yet accurate, analysis. Part two describes the application of developed theory to most commonly used geometries of thin-walled, open-section composite beams.

1. Introduction

Thin-walled composite beams have become an integral part of many engineering structures today. The technology, which evolved mainly from the aerospace industry (e.g., rocket motor casings, space booms, rotor blades, etc.), finds its application in fields as diverse as sports (e.g., skis, tennis rackets, golf clubs, etc.), sea hulls, offshore rigs, automotive components (e.g., power transmission shafts), and architecture (e.g., I-section beams, channel-section beams, etc.). Despite their superior engineering properties and enhanced manufacturing technology, their development is not up to their potential due to cost considerations. One of the sure ways to reduce development cost is to establish accurate analysis tools to aid in tailoring of composite structures. In particular, analytical tools that can be used in preliminary design and efficient numerical tools that can be used in detailed design are of prime importance.

Existing classical analytical tools suffice for most simple structures. However, many important practical phenomena have been observed in thin-walled beams to which these classical tools are blind. The effects being dealt with in this work are non-classical nonlinear effects. We begin with the introduction and definitions of some terminology.

Physical nonlinearities are basically nonlinearities in the stress-strain relationship becoming important by virtue of strain being large. Geometrical nonlinearities, on the other hand, are nonlinearities in the strain-displacement relationship becoming important by virtue of rotation being (at least moderately) large. A nonlinear beam theory could arise either due to 1-D physical nonlinearities or 1-D geometric nonlinearities or both. Certain 1-D physical nonlinearities occur because of 3-D geometric nonlinearities (large 3-D warping), and these are called non-classical nonlinearities. Composite open-section beams have low torsional rigidity and hence allow fairly large twist rates, not only due to torsion but also to coupling with other types of loading that accentuate the importance of nonlinearities involving twist. These effects are important in the case of thin-walled beams, but in an asymptotic sense they are not so important in the cases of beams with solid or thick-walled sections. Summarizing, in slender structures

☆ A part of this paper was published at 49th AIAA Structures, Structural Dynamics, & Materials Conference, Schaumburg, IL, USA, Apr 7–10 (2008).

* Corresponding author.
E-mail addresses: dinesh@aero.iisc.ernet.in (D. Harursampath), harish@ikm.uni-hannover.de (A.B. Harish), dhodges@gatech.edu (D.H. Hodges).

http://dx.doi.org/10.1016/j.tws.2017.03.018
Received 28 October 2015; Received in revised form 18 December 2016; Accepted 14 March 2017
Available online 22 May 2017

Nomenclature

x_1	Cartesian coordinate along the reference axis of a beam
x_i	Cartesian coordinates for a cross section, $i = 2, 3$
$\mathbf{b}_i$	unit vectors for undeformed geometry, $i = 1, 2, 3$
$\mathbf{B}_i$	unit vectors for deformed geometry, $i = 1, 2, 3$
q_i	rigid-body-like displacements of a cross section, $i = 1, 2, 3$
Γ_{ij}	3-D strains, $i, j = 1, 2, 3$
σ_{ij}	3-D stresses, $i, j = 1, 2, 3$
E^{ijkl}	3-D stiffness constants, $i, j, k, l = 1, 2, 3$
$\epsilon_{\alpha\beta}$	2-D membrane strains, $\alpha, \beta = 1, 2$
$\rho_{\alpha\beta}$	2-D elastic curvatures, $\alpha, \beta = 1, 2$
A_{ij}	2-D membrane stiffness constants, $i, j = 1, 2, 6$
B_{ij}	2-D coupling stiffness constants, $i, j = 1, 2, 6$
D_{ij}	2-D bending/twisting stiffness constants, $i, j = 1, 2, 6$
γ_{11}	1-D axial strain
κ_1	1-D elastic twist per unit length
κ_i	1-D elastic bending curvatures, $i, j = 2, 3$
S	1-D stiffness matrix
$\overline{w}_i$	warping of a cross section, $i = 1$ (out-of-plane), $i = 2, 3$ (in-plane)
ℓ	characteristic wavelength of a beam
b	characteristic dimension of a cross section
h	thickness of a thin wall
k_1	initial twist per unit length of beam
k_2	initial flatwise curvature of a strip
δ_h	small parameter, $\frac{h}{b}$
δ_b	small parameter, $\frac{b}{\ell}$
δ_t	small parameter, bk_1
ϵ	small parameter, magnitude of largest Γ_{ij}
N_s	total number of strips making up an open-section beam
N_j	total number of joints in an open-section beam
$N_c(m)$	number of strips connected at m-th joint

undergoing motions with large wavelengths, these nonlinear and non-classical effects may play a significant role. Moreover, additional refinements are required to enhance the accuracy of the solution in the following cases: (a) Timoshenko refinement is required when short wavelength modes associated with transverse shear are involved; (b) Vlasov refinement is required for thin-walled, open-section beams, as captured in the current work; and (c) general refinements are required when new degrees of freedom are introduced particular to the problem – such as high-frequency vibrations.

The current work is motivated by the need for a general-purpose tool to capture the non-classical effects of thin-walled, open-section composite beams in closed-form via an asymptotic method. It is focused at developing analytical solutions incorporating nonlinear strain fields, which are the sources of many such effects. This work addresses non-classical effects observed in thin-walled, open-section beams that can be considered as a pretwisted assembly of strips. The primary 3-D sources of nonlinearity in such a beam stem from the out-of-plane cross-sectional warping. This 3-D nonlinearity manifests as two well-known non-classical effects, namely Trapeze and Vlasov effects.

Before proceeding ahead, it is important to understand the classification of beams as discussed in [26]. As per the nomenclature used in this work, beams are classified into T-class, S-class and R-class. Consider the characteristic length along the thickness is h and along the cross-sectional plane is a. T-class refers to the thin-walled, open-section beams that is of primary importance to this work. T-class beams are torsionally soft, in comparison to bending, since the strain induced by twisting is $O(h\kappa_1)$, while the strain induced by bending is $O(a\kappa_2)$ or $O(a\kappa_3)$. S-class beams are strip-like with $a >> ha >> h$. These beams are soft in torsion and also in one bending direction. High aspect-ratio wings, helicopter blades etc fall into this category. Finally, the R-class beams are the regular beams that are neither T-class nor S-class and do not demonstrate significant length effects. Some examples are closed-cell, solid, closed-section beams.

Thin-walled composite beams are widely favored in aerospace structures. Examples of sections that can be analyzed using the present work include I-sections, T-sections, X-sections, Z-sections, cruciforms, and any custom section that can be constructed from an assembly of arbitrarily oriented straight elements. Though 3-D finite element modeling of such beams is possible, it is computationally expensive when modeling large structures. Existing classical analytical tools suffice for most simple structures. However, many important practical phenomenon have been observed in thin-walled composite as well as isotropic beams to which classical tools are blind. Many existing 1-D models make *ad hoc* assumptions for thin-walled beams and neglect the non-classical effects.

This work takes advantage of the beam-like configuration, which allows consideration of the ratio between a characteristic cross-sectional dimension and the wavelength of the deformation along the beam as a small parameter. The non-linear 3-D problem is decomposed into two simpler problems: a two-dimensional (2-D) nonlinear analysis, which provides in a compact form the cross-sectional properties using a mathematical technique called the Variational-Asymptotic Method (VAM), and a nonlinear one-dimensional (1-D) problem along the length of the beam. The results from the former analysis act as inputs to the latter, and both may be highly nonlinear. Owing to this decomposition, a major simplification ensues in the complex 3-D problem. This efficient approach to the structural analysis of beams is outlined as a flowchart in Fig. 1.

The nonlinear cross-sectional analysis provides stiffness coefficients along with recovery relations, which are functions of the generalized 1-D strain measures. The stiffness coefficients are needed to solve the 1-D beam problem. Solving the 1-D problem, one obtains the 1-D displacements and generalized strain measures. After both problems have been solved, the in-plane and out-of-plane warping of the cross section, the total 3-D displacement field, and the 3-D strain and stress fields can all be recovered.

VAM also brings into importance the concept of asymptotic correctness. The theoretical or numerical solutions obtained are approximate in nature. Accuracy of the numerical solutions are asserted by reduction in relative error norms (or otherwise often referred to as

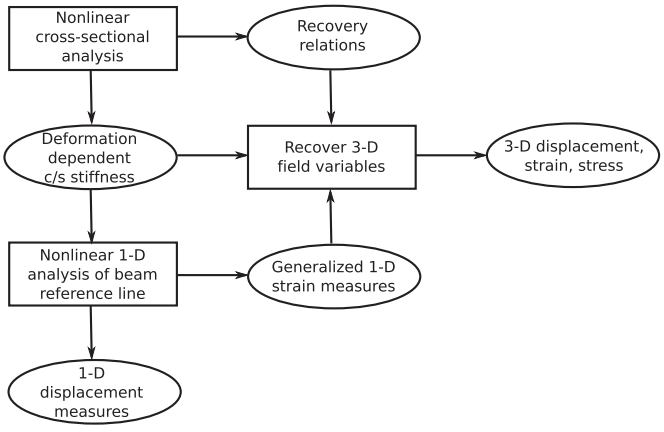

Fig. 1. Procedure for beam analysis.

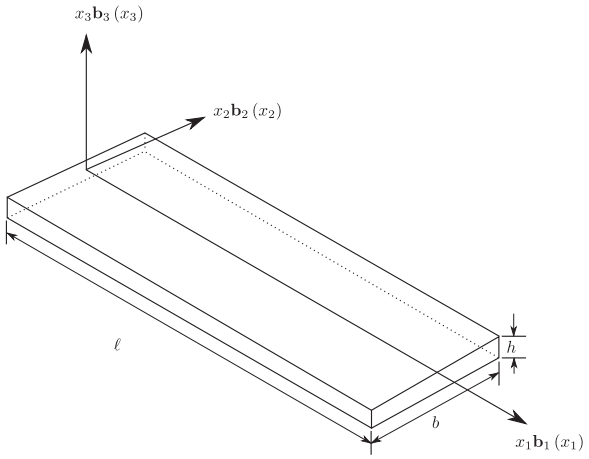

Fig. 2. Pretwisted strip configuration and coordinate system.

convergence). Similarly, asymptotic correctness can be defined as a measure of the accuracy of the theoretical (approximate) solutions. Quoting verbatim from [44], *asymptotic correctness concerning an approximate solution denotes its agreement to a specified order in a small parameter with an asymptotic expansion of the exact solution in that parameter*. Overall, this works provides an effective mathematical framework for development of tools to assist composite tailoring of thin-walled, open-section composite beams.

2. Review of earlier works

Modeling of beam-like anisotropic structures having arbitrary geometry in terms of initial curvature, pretwist and cross-sectional shape has been the focus of several previous works by Hodges et al. [27], Cesnik and Hodges [11], Cesnik et al. [14] and Cesnik and Hodges [12]. The resulting asymptotically-correct solutions have been implemented in commercial software called VABS (Variational-Asymptotic Beam Section) by Cesnik and Hodges [13] and later updated by Yu et al. [51,52].

VAM was originally developed by Berdichevsky for shells in Berdichevsky [3] and beams in Berdichevsky [4] and further on introducing shear effects in Berdichevsky and Starosel'skii [6]. This technique has been applied to thin-walled closed [5] and open [2,47] cross section anisotropic beams, with linear shell theory as the starting point, resulting in closed-form solutions for the classical coefficients. Overall, VAM provides a dimensional reduction of the 3-D nonlinear problem into a 1-D nonlinear problem by taking advantage of the small parameters of the problem. Several works have been presented since then expanding the applicability of VAM and to study nonlinear and non-classical effects observed in aerospace structures. Volovoi [43] used VAM for the first time to analyze end effects for prismatic anisotropic beams with thin-walled open cross sections, but his analysis was strictly linear. However, linearity precludes a cross-sectional analysis from capturing many of the non-classical phenomena, such as trapeze and Brazier effects, which are of well-known importance in rotor blades and tube bending, respectively. Harursampath and Hodges [23] applied VAM for nonlinear cross-sectional analysis of composite tubular beams, extracting the non-classical Brazier effect.

The trapeze effect is fundamentally a nonlinear coupling of extension and twist. In rotor blade analyses it is frequently exhibited as a linear term that increases the effective torsional rigidity as a function of axial force; see, for example, Hodges and Dowell [28]. This term is not contained in the exact intrinsic equilibrium equations for a beam, for example, those of Reissner [39]. Therefore, it *must* enter the analysis through the constitutive law.

Buckley [10] first explained the trapeze effect by considering the isotropic beam as being composed of a number of longitudinal material fibers. Wagner [48] applied this concept to analyze torsional buckling. This hypothesis is presently used by many helicopter blade analysis tools. Biot [7] used second order rotation effects in conjunction with a state of prestress. Following the method, Goodier [21] considered Trefftz stress components and determined the influence of bending on torsional rigidity. Houbolt and Brooks [30] incorrectly (see [24,40]) derived the effect of pretwist. Hodges [24] recognized the source of the trapeze effect to be the non-linear strain field. Danielson and Hodges [16] then devised a systematic procedure to obtain the nonlinear strain field for a general case. The most general cross-sectional analysis in which the nonlinear terms needed to model this effect are included is the work of Borri and Merlini [9] who developed these terms from a "geometric stiffness" point of view. Armanios et al. [1] derived the asymptotic extension-twist relation for an antisymmetric pretwisted strip. The trapeze effect has also been treated in the analytical treatments of Berdichevsky [4]. Popescu [34] was the first to employ VAM with geometrically non-linear theory as the starting point for a *numerical treatment* of the trapeze effect of general solid beams. Hodges et al. [29] were the first to do the same for an *analytical treatment*, but it was restricted to strips. Popescu and Hodges [35] considered numerical treatment of nonlinear effects (such as the Trapeze effect) through cross-sectional analysis.

Volovoi et al. [46] analyzed Vlasov effect in thin-walled open-section beams using VAM and demonstrated classical laminated plate theory to be an effective starting point. Volovoi and Hodges [44] generalized the work of Volovoi et al. [46] to provide linear asymptotically correct theory for thin-walled beams of arbitrary cross section and demonstrated insignificance of Vlasov effect in closed-section beams. Volovoi and Hodges [45] considered single and multi-cell configurations to incorporate the shell bending strain measures into the formulation. Yu et al. [54] provide a general framework to model thin-walled general cross section composite beams as a possible alternative to VABS approach. However, this work does not consider the Vlasov or shear deformation effects. Yu et al. [53] address issues pertaining to Vlasov correction for increasing the accuracy of beam theory, which are incorporated into VABS for thin-walled open-section beams. Roy and Yu [41] further extended the work of Yu et al. [53] to account for both pretwist and initial curvature in thin-walled general cross section beams.

Popescu and Hodges [36] extended the classical theory comprising extension, torsion and bending to include transverse shear terms in 1-D analysis using VAM. Popescu et al. [37] showed that obliqueness can be considered as a small parameter in VAM. Hodges [25] presents an intrinsic formulation to consider the dynamics of curved and twisted anisotropic beams. Palacios and Cesnik [33] further discuss solution methods for solving the 1-D nonlinear dynamic problem for slender beams by coupling VAM with FEM. Sotoudeh and Hodges [42] discuss solution strategies for the intrinsic 1-D nonlinear equations subjected to various boundary conditions. Alternatively, Yu et al. [52] provided a FE-based cross-sectional analysis of pretwisted beams inclusive of classical and non-classical coupling effects. A comparison between the 3-D elasticity-based solutions and those obtained from VAM for Euler-Bernoulli-like and Timoshenko-like beams can be found in Yu and Hodges [50].

VAM has also been further applied to several multiphysics problems, including thermo-elastic [49]) and electro-elastic [32] problems, related to conventional and smart slender structures.

There have been several works based on Finite Element solutions for thin-walled composite beams. Some of the latest works include those of Genoese et al. [20,19], Garceaa et al. [18], Gabriele et al. [17], Nguyen et al. [31]. Genoese et al. [20] proposes a mixed linear model based on the Hellinger-Reissner mixed variational principle for heterogeneous materials, including warping and section distortion. The solution is based on a polynomial part and extended to include tip effects through an exponential part. Further on, Genoese et al. [19] apply the same implicit co-rotational technique to describe complex 3D effects caused by nonuniform warping and to analyze buckling of beams.

3. Analytical development

In this section, the foundation is laid for developing a rigorous non-classical nonlinear asymptotic theory for beams which could be considered as an arbitrary assembly of thin, rectangular members subjected to pretwist. A thin, pretwisted composite strip is modeled as a beam, including those nonlinear effects that need to be considered, by virtue of the special geometry, to establish asymptotic correctness. This is achieved by deriving its strain energy function in terms of 1-D quantities only. A geometrically nonlinear laminated shell theory is derived, and VAM is used as a tool to carry out the dimensional reduction from 2-D to 1-D. The analysis is generically performed for each strip in the open section beam, and finally cumulative effects of all the strips are considered to obtain the properties of the beam.

Analytical expressions are presented in this section for the non-classical non-linear 1-D stiffness, 3-D stress and warping fields for pretwisted open-section thin-walled beams. The only restriction is that it should be possible to model the beam as a pretwisted assembly of thin rectangular strips rigidly joined to each other with an overall cross-sectional aspect ratio of the order of unity. Any number of arbitrarily inclined strips of different sizes, layups and materials can be connected at joints. Moreover, the joints could be located anywhere along the strips.

3.1. Undeformed geometry

Asymptotic methods require small parameters. Here the wavelength of deformation along the strip is denoted by ℓ. The width and thickness of the strip are denoted by b and h respectively. From the geometry of the strip, the natural small parameters are the thickness-to-width ratio $\delta_h = h/b$; the width-to-length ratio $\delta_b = b/\ell$; and the width times the pretwist per unit length $\delta_t = bk_1$, where $k_1(x_1)$ is the derivative of the pretwist angle with respect to length along the strip. The geometry of the strip is as shown in Fig. 2. The Cartesian coordinate system measures x_i are directed along the length, width and thickness of the strip for $i=1$, 2 and 3, respectively, parallel to corresponding unit vectors $\mathbf{b}_i$.

The domain of each component of the strip-beam in Fig. 2 is such that $0 \le x_1 \le l$, $-\frac{b}{2} \le x_2 \le \frac{b}{2}$ and $-\frac{h}{2} \le x_3 \le \frac{h}{2}$. The position vector from a point fixed in an inertial reference frame a to a generic point on the middle surface of the strip is $\mathbf{r} = x_1\mathbf{b}_1 + x_2\mathbf{b}_2(x_1)$. The position vector of an arbitrary material point in the undeformed strip is then

$$\check{\mathbf{r}} = \mathbf{r} + x_3\mathbf{b}_3(x_1) = x_i\mathbf{b}_i \tag{1}$$

The position vector $\check{\mathbf{R}}(x_1, x_2, x_3)$ of an arbitrary material point in the deformed configuration is given by

$$\begin{aligned}\check{\mathbf{R}} &= x_1\mathbf{b}_1 + q_i(x_1)\mathbf{b}_i + x_2\mathbf{B}_2(x_1)\\ &\quad + x_3\mathbf{B}_3(x_1) + \overline{w}_i(x_1, x_2, x_3)\mathbf{B}_i(x_1)\end{aligned} \tag{2}$$

where q_i are rigid-body-like displacements; $\mathbf{B}_i$ are orthogonal unit vectors introduced by rigid-body-like rotation; and $\overline{w}_i$ are warping displacements of the beam cross section.

The covariant and contravariant base vectors for the undeformed state, $\mathbf{g}_i$ and $\mathbf{g}^i$; the covariant base vectors for the deformed state, $\mathbf{G}_i$; the deformation gradient, $\overline{\mathbf{F}} = \mathbf{G}_i\mathbf{g}^i$; the 3-D strains, Γ_{ij}; relations between the 2-D (shell) strain measures, (ϵ_{11}, ϵ_{22}, ϵ_{12}, ρ_{11}, ρ_{22}, ρ_{12}), and the 1-D (beam) strain measures, (γ_{11}, κ_1, κ_2, κ_3); the warping displacements, w_i; and an explanation of the order of magnitude analyses are all directly taken from the work of Hodges and co-workers [29].

The 3-D strain measures are asymptotically related to the 2-D strain measures for thin shells by $\Gamma_{\alpha\beta} = \epsilon_{\alpha\beta} + x_3\rho_{\alpha\beta}$ where $\epsilon_{\alpha\beta}$ are the membrane strains and $\rho_{\alpha\beta}$ are the middle surface bending curvatures. Hence, as discussed in the work of Hodges and co-workers [29], we can write the relation between 2-D (shell) measures and the 1-D (beam) measures. The membrane strains are

$$\begin{aligned}\epsilon_{11} &\approx \gamma_{11} - x_2\kappa_3 + k_1x_2^2\kappa_1 + \underline{\frac{x_2^2\kappa_1^2}{2}} + \underline{w_3\kappa_2}\\ \epsilon_{22} &\approx w_{2,2} + \underline{\frac{1}{2}w_{3,2}^2}\\ 2\epsilon_{12} &\approx w_{1,2} + k_1(x_2w_{3,2} - w_3) + \underline{\kappa_1(x_2w_{3,2} - w_3)}\end{aligned} \tag{3}$$

while the curvatures are

$$\begin{aligned}\rho_{11} &\approx \kappa_2\\ \rho_{22} &\approx -w_{3,22}\\ 2\rho_{12} &\approx -2\kappa_1\end{aligned} \tag{4}$$

The strain measures in Eqs. (3) and (4) can be rewritten showing the respective order-of-magnitude estimates as

$$\begin{aligned}\epsilon_{11} &= \underbrace{\gamma_{11} - x_2\kappa_3 + k_1x_2^2\kappa_1}_{O(\epsilon)} + \underbrace{\frac{x_2^2\kappa_1^2}{2} + w_3^0\kappa_2}_{O(\epsilon\Delta)} + \underbrace{\widetilde{w}_3\kappa_2}_{O(\epsilon\Delta^2)}\\ \epsilon_{12} &= \underbrace{\epsilon_{12}^0}_{O(\epsilon)} + \underbrace{\widetilde{\epsilon}_{12}}_{O(\epsilon\Delta)}\\ \epsilon_{22} &= \underbrace{\epsilon_{22}^0}_{O(\epsilon)} + \underbrace{\widetilde{\epsilon}_{22}}_{O(\epsilon\Delta)}\\ \rho_{11} &= \underbrace{\kappa_2}_{O(\epsilon)}\\ \rho_{22} &= \underbrace{-w_{3,22}^0}_{O(\epsilon)} - \underbrace{\widetilde{w}_{3,22}}_{O(\epsilon\Delta)}\\ 2\rho_{12} &= \underbrace{-2\kappa_1}_{O(\epsilon)}\end{aligned} \tag{5}$$

The 2-D strain energy can be written in terms of the membrane strains and curvatures as

$$U_{2D} = \frac{1}{2}\left\{\begin{matrix}\epsilon\\ \rho\end{matrix}\right\}\left[\begin{matrix}A & B\\ B & D\end{matrix}\right]\left\{\begin{matrix}\epsilon\\ \rho\end{matrix}\right\} \tag{6}$$

where A, B and D refer to the membrane, coupling and bending stiffness matrices from Classical Laminated Plate theory and for which explicit expressions can be found in [38]. The membrane strains and curvatures can be expressed in terms of 1-D strains and warping, and minimization can be performed, as described below, to determine the unknown warping functions.

The zeroth-order approximation to the 2-D strain energy consists of all terms of $O(E\epsilon^2)$, thus leading to the asymptotic classical linear

theory for generally anisotropic pretwisted rectangular strips. Hence, the zeroth-order approximations to the 2-D membrane and bending strains are all of the non-underlined terms ($O(\epsilon)$) in Eqs. (3) and (4), respectively. All zeroth-order variables will be denoted by a subscript 0. Minimization of the zeroth-order strain energy leads to ϵ_{12}^0 (the only strain measure that has a w_1^0-dependent term), ϵ_{22}^0 (the only strain measure that has a w_2^0-dependent term) and ρ_{22}^0(the only strain measure that has a w_3^0-dependent term) being expressed in terms of the other known 2-D strain measures. Closed-form solutions are then obtained for the zeroth-order warping displacements w_i^0 and it is verified that their orders of magnitude agree with our estimations.

The first-order approximation to the 2-D strain energy consists of all terms of $O(E\epsilon^2)$, $O(E\epsilon^2\Delta)$ and $O(E\epsilon^2\Delta^2)$. Hence, the first-order approximations to the 2-D strains should contain all terms up to $O(\epsilon\Delta^2)$. This consists of both the underlined and non-underlined terms in Eqs. (3) and (4). First-order variables will be denoted by the superscript *I*. The warping displacements are given by $w_i^I = w_i^0 + \widetilde{w}_i$, where the perturbation quantities $\widetilde{w}_i$ are assumed to be of one order higher than the corresponding zeroth-order quantities, w_i^0. Thus, $\widetilde{w}_\alpha = O(\epsilon\Delta b)$ and $\widetilde{w}_3 = O\left(\frac{\epsilon\Delta b}{\delta_h}\right)$.

Minimization with respect to the three unknowns $\tilde{\epsilon}_{12}$, $\tilde{\epsilon}_{22}$ and $\tilde{\rho}_{22}$ is equivalent to minimization with respect to $\widetilde{w}_i$ and is conducted in three steps:

1. Only the terms of order $\epsilon^2\Delta^2$ are retained upon the substitution of Eq. (5) into the energy.
2. ϵ_{12}^I (the only strain measure that has a $\widetilde{w}_1-$dependent term) and ϵ_{22}^I (the only strain measure that has a $\widetilde{w}_2-$dependent term) are expressed in terms of the other 2-D strain measures.
3. These expressions are substituted into the first-order strain energy functional, and the result is minimized with respect to $\widetilde{w}_3$, subject to the appropriate constraints.

Closed-form solutions are then obtained for the perturbations to the zeroth-order warping displacements w_i^0, and it is verified that their orders of magnitude agree with our estimations.

3.2. Pretwisted open-section thin-walled beams

Fig. 3 shows a typical component strip in the undeformed configuration. The beam reference line can be chosen, for example, as the locus of cross-sectional centroids, *O*. At any given cross section, the 1-D curvature vector, with components κ_i, then passes through *O*. Each component strip is identified by an index, $n\,(n = 1,\ldots,N_s)$. Each joint of two or more strips is identified by an index, $m\,(m = 1,\ldots,N_j)$. The same notations as those used for the single pretwisted strip-beam, but with the subscript *n*, are used here for the geometrical properties of the *n*-th strip. In the undeformed configuration, the unit vector $\mathbf{b}_{n2}$ along the width of the *n*-th strip is inclined at an angle α_n to $\mathbf{b}_2$ and the centroid of the *n*-th strip is displaced from the cross-sectional centroid *O* by $X_{n2}\mathbf{b}_2 + X_{n3}\mathbf{b}_3$, where $\mathbf{b}_2$ and $\mathbf{b}_3$ are unit vectors associated with the cross section. In this section, repeated indices are *not* summed over their ranges unless explicitly stated.

3.2.1. 1-D stiffness

The 1-D strain energy density of open section beam is

$$U_{1D} = \frac{1}{2}\begin{Bmatrix}\gamma_{11}\\ \kappa_1\\ \kappa_2\\ \kappa_3\\ \kappa_1^2\\ \kappa_1'\end{Bmatrix}^T [S] \begin{Bmatrix}\gamma_{11}\\ \kappa_1\\ \kappa_2\\ \kappa_3\\ \kappa_1^2\\ \kappa_1'\end{Bmatrix} \tag{7}$$

where $[S]$ is the 6×6 stiffness matrix. The fifth row and column of $[S]$ correspond to nonlinearities contributed by large elastic twist while the sixth row and column correspond to the end effects contributed by large elastic twist. Both are non-classical effects brought into prominence by the existence of small geometric parameters in thin-walled open-section beams.

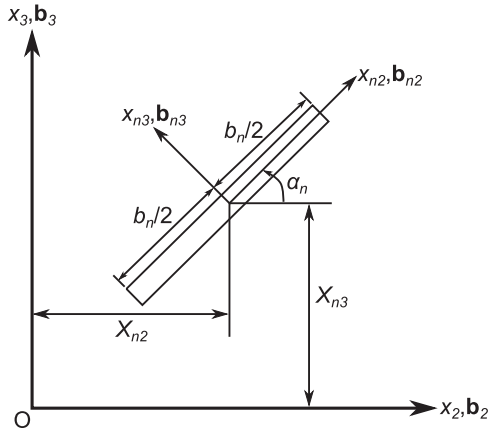

Fig. 3. Component strip configuration and coordinate system.

The first four rows and columns contain the classical stiffness coefficients:

$$\begin{aligned}
S_{11} &= \sum_{n=1}^{N_s} b_n \overline{A}_{11}^n \\
S_{12} &= -2\sum_{n=1}^{N_s} b_n \overline{B}_{16}^n + k_1 \sum_{n=1}^{N_s} b_n\left(\frac{b_n^2}{12} + X_{n2}^2 + X_{n3}^2\right)\overline{A}_{11}^n \\
S_{13} &= \sum_{n=1}^{N_s} b_n X_{n3} \overline{A}_{11}^n \\
S_{14} &= -\sum_{n=1}^{N_s} b_n X_{n2} \overline{A}_{11}^n \\
S_{22} &= 4\sum_{n=1}^{N_s} b_n \overline{D}_{66}^n - k_1 \sum_{n=1}^{N_s} b_n\left[\frac{b_n^2}{3} + 4(X_{n2}^2 + X_{n3}^2)\right]\overline{B}_{16}^n \\
&\quad + k_1^2 \sum_{n=1}^{N_s} b_n\left[\frac{b_n^4}{80} + (X_{n2}^2 + X_{n3}^2)\left(\frac{b_n^2}{6} + X_{n2}^2 + X_{n3}^2\right)\right. \\
&\quad \left. + b_n^2\frac{(\cos\alpha_n X_{n2} + \sin\alpha_n X_{n3})^2}{3}\right]\overline{A}_{11}^n \\
S_{23} &= -2\sum_{n=1}^{N_s} b_n X_{n3}\overline{B}_{16}^n + k_1 \sum_{n=1}^{N_s} \\
&\quad \times b_n\left[b_n^2\left(\frac{X_{n3}}{6} + \frac{\sin 2\alpha_n X_{n2} - \cos 2\alpha_n X_{n3}}{12}\right) + X_{n3}(X_{n2}^2 + X_{n3}^2)\right]\overline{A}_{11}^n \\
S_{24} &= 2\sum_{n=1}^{N_s} b_n X_{n2}\overline{B}_{16}^n - k_1 \sum_{n=1}^{N_s} \\
&\quad \times b_n\left[b_n^2\left(\frac{X_{n2}}{6} + \frac{\sin 2\alpha_n X_{n3} + \cos 2\alpha_n X_{n2}}{12}\right) + X_{n2}(X_{n2}^2 + X_{n3}^2)\right]\overline{A}_{11}^n
\end{aligned} \tag{8}$$

$$\begin{aligned}
S_{33} &= \sum_{n=1}^{N_s} b_n\left(\sin^2\alpha_n\frac{b_n^2}{12} + X_{n3}^2\right)\overline{A}_{11}^n \\
S_{34} &= -\sum_{n=1}^{N_s} b_n\left(\sin 2\alpha_n\frac{b_n^2}{24} + X_{n2}X_{n3}\right)\overline{A}_{11}^n \\
S_{44} &= \sum_{n=1}^{N_s} b_n\left(\cos^2\alpha_n\frac{b_n^2}{12} + X_{n2}^2\right)\overline{A}_{11}^n
\end{aligned}$$

The elements of the fifth row and column of $[S]$ are as follows:

$$
\begin{aligned}
S_{15} &= \sum_{n=1}^{N_s} \frac{b_n}{2}\left(\frac{b_n^2}{12} + X_{n2}^2 + X_{n3}^2\right)\overline{A}_{11}^n \\
S_{25} &= -\sum_{n=1}^{N_s} b_n\left(\frac{b_n^2}{12} + X_{n2}^2 + X_{n3}^2\right)\overline{B}_{16}^n \\
&\quad + k_1\sum_{n=1}^{N_s} \frac{b_n}{2}\left[\frac{b_n^4}{80} + (X_{n2}^2 + X_{n3}^2)\left(\frac{b_n^2}{6} + X_{n2}^2 + X_{n3}^2\right)\right. \\
&\quad \left. + b_n^2\frac{(\cos\alpha_n X_{n2} + \sin\alpha_n X_{n3})^2}{3}\right]\overline{A}_{11}^n \\
S_{35} &= \sum_{n=1}^{N_s} b_n\left[b_n^2\left(\frac{X_{n3}}{12} + \frac{\sin 2\alpha_n X_{n2} - \cos 2\alpha_n X_{n3}}{24}\right)\right. \\
&\quad \left. + \frac{X_{n3}}{2}(X_{n2}^2 + X_{n3}^2)\right]\overline{A}_{11}^n \\
S_{45} &= -\sum_{n=1}^{N_s} b_n\left[b_n^2\left(\frac{X_{n2}}{12} + \frac{\sin 2\alpha_n X_{n3} + \cos 2\alpha_n X_{n2}}{24}\right)\right. \\
&\quad \left. + \frac{X_{n2}}{2}(X_{n2}^2 + X_{n3}^2)\right]\overline{A}_{11}^n \\
S_{55} &= \sum_{n=1}^{N_s} \frac{b_n}{4}\left[\frac{b_n^4}{80} + (X_{n2}^2 + X_{n3}^2)\left(\frac{b_n^2}{6} + X_{n2}^2 + X_{n3}^2\right)\right. \\
&\quad \left. + b_n^2\frac{(\cos\alpha_n X_{n2} + \sin\alpha_n X_{n3})^2}{3}\right]\overline{A}_{11}^n
\end{aligned} \tag{9}
$$

Note that the nonlinear extension-twist coupling $S_{15} > 0$ under all circumstances (material or geometry) indicating the importance of the trapeze effect in all isotropic/composite twisted/untwisted thin-walled open-section beams even if the linear extension-twist coupling stiffness $S_{12} = 0$, which happens for symmetric layups with no pretwist. In other words, an extensional load invariably causes torsional stiffening.

The elements of the sixth row and column of $[S]$ are as follows:

$$
\begin{aligned}
S_{16} &= \sum_{n=1}^{N_s} b_n c_n \overline{A}_{11}^n \\
S_{26} &= -2\sum_{n=1}^{N_s} b_n c_n \overline{B}_{16}^n \\
&\quad + k_1\sum_{n=1}^{N_s} b_n\left[c_n\left(\frac{b_n^2}{12} + X_{n2}^2 + X_{n3}^2\right)\right. \\
&\quad \left. - \sin 2\alpha_n b_n^2\frac{X_{n2}^2 - X_{n3}^2}{12} + \cos 2\alpha_n\frac{b_n^2 X_{n2}X_{n3}}{6}\right]\overline{A}_{11}^n \\
S_{36} &= \sum_{n=1}^{N_s} b_n\left(c_n X_{n3} + \sin\alpha_n b_n^2\frac{\cos\alpha_n X_{n3} - \sin\alpha_n X_{n2}}{12}\right)\overline{A}_{11}^n \\
S_{46} &= -\sum_{n=1}^{N_s} b_n\left(c_n X_{n2} + \cos\alpha_n b_n^2\frac{\cos\alpha_n X_{n3} - \sin\alpha_n X_{n2}}{12}\right)\overline{A}_{11}^n \\
S_{56} &= \sum_{n=1}^{N_s} \frac{b_n}{2}\left[c_n\left(\frac{b_n^2}{12} + X_{n2}^2 + X_{n3}^2\right)\right. \\
&\quad \left. - \sin 2\alpha_n b_n^2\frac{X_{n2}^2 - X_{n3}^2}{12} + \cos 2\alpha_n\frac{b_n^2 X_{n2}X_{n3}}{6}\right]\overline{A}_{11}^n \\
S_{66} &= \sum_{n=1}^{N_s} b_n\left[c_n^2 + b_n^2\frac{(\sin\alpha_n X_{n2} - \cos\alpha_n X_{n3})^2}{12}\right]\overline{A}_{11}^n
\end{aligned} \tag{10}
$$

where the constants $c_n (n = 1,\ldots,N_s)$ need to be solved for from the following simultaneous linear equations:

$$
\begin{aligned}
\sum_{n=1}^{N_s} b_n c_n &= 0 \\
c_p + x_{p2}(m)(\cos\alpha_p X_{p3} - \sin\alpha_p X_{p2}) &= c_q + x_{q2}(m)(\cos\alpha_q X_{q3} - \sin\alpha_q X_{q2}) \\
&\quad (m = 1,\ldots,N_j)
\end{aligned} \tag{11}
$$

The second of the above equations is for the intersection of the p-th and the q-th strip at the m-th joint. It results from the continuity of the leading term in the out-of-plane warping of the strips at the joint. If $N_c(m) \geq 2$ is the total number of strips connected at the m-th joint, the second equation above repeats itself $N_c(m) - 1$ times at this joint. The notation $x_{p2}(m)$ refers to the local x_2 coordinate of the m-th joint of the p-th strip.

The stiffness variables $\overline{\overline{A}}_{11}^n$, $\overline{\overline{B}}_{16}^n$ and $\overline{\overline{D}}_{66}^n$ which are used in expressing the 1-D stiffness matrix can be given for a component strip numbered $n (n = 1,\ldots,N_s)$ as

$$
\begin{aligned}
\overline{\overline{A}}_{11}^n\Delta^n &= A_{11}^n\Delta^n - 2A_{12}^nA_{66}^nB_{12}^nB_{22}^n - A_{16}^{n\,2}B_{22}^{n\,2} \\
&\quad + 2A_{12}^nA_{16}^nB_{22}^nB_{26}^n - A_{12}^{n\,2}B_{26}^{n\,2} + A_{12}^{n\,2}A_{66}^nD_{22}^n \\
&\quad - A_{26}^{n\,2}B_{12}^{n\,2} \\
&\quad + A_{22}^n(A_{66}^nB_{12}^{n\,2} - 2A_{16}^nB_{12}^nB_{26}^n + A_{16}^{n\,2}D_{22}^n) \\
&\quad + 2A_{26}^n(A_{12}^nB_{12}^nB_{26}^n + A_{16}^nB_{12}^nB_{22}^n - A_{16}^nA_{12}^nD_{22}^n) \\
\overline{\overline{B}}_{16}^n\Delta^n &= B_{16}^n\Delta^n - A_{12}^nB_{26}^{n\,3} + A_{16}^nB_{22}^nB_{26}^{n\,2} - A_{16}^nB_{22}^{n\,2}B_{66}^n \\
&\quad - A_{22}^nB_{12}^nB_{26}^nB_{66}^n + A_{12}^nB_{22}^nB_{26}^nB_{66}^n + A_{16}^nA_{22}^nB_{66}^nD_{22}^n \\
&\quad - A_{16}^nA_{22}^nB_{26}^nD_{26}^n - A_{26}^{n\,2}B_{12}^nD_{26}^n \\
&\quad + A_{66}^n[B_{26}^n(A_{12}^nD_{22}^n - B_{12}^nB_{22}^n) \\
&\quad + D_{26}^n(A_{22}^nB_{12}^n - A_{12}^nB_{22}^n)] \\
&\quad + A_{26}^n(B_{12}^nB_{26}^{n\,2} + B_{12}^nB_{22}^nB_{66}^n \\
&\quad - A_{16}^nB_{26}^nD_{22}^n - A_{12}^nB_{66}^nD_{22}^n) \\
&\quad + (A_{16}^nB_{22}^n + A_{12}^nB_{26}^n)D_{26}^nA_{26}^n \\
\overline{\overline{D}}_{66}^n\Delta^n &= D_{66}^n\Delta^n - B_{26}^{n\,4} - B_{66}^{n\,2}(B_{22}^{n\,2} - A_{22}^nD_{22}^n) \\
&\quad + 2A_{26}^nB_{22}^nB_{66}^nD_{26}^n - (A_{26}^{n\,2} - A_{22}^nA_{66}^n)D_{26}^{n\,2} \\
&\quad + B_{26}^{n\,2}(2B_{22}^nB_{66}^n + A_{66}^nD_{22}^n + 2A_{26}^nD_{26}^n) \\
&\quad - 2B_{26}^n(A_{66}^nB_{22}^nD_{26}^n + B_{66}^nA_{26}^nD_{22}^n + B_{66}^nA_{22}^nD_{26}^n)
\end{aligned} \tag{12}
$$

where

$$
\Delta^n = -2A_{26}^nB_{22}^nB_{26}^n + A_{22}^nB_{26}^{n\,2} + A_{26}^{n\,2}D_{22}^n + A_{66}^n(B_{22}^{n\,2} - A_{22}^nD_{22}^n) \tag{13}
$$

A^n, B^n and D^n refer to the membrane, coupling and bending stiffness matrices of the n-th strip from Classical Laminated Plate theory, for which explicit expressions can be found, for instance, in [38].

3.2.2. 3-D stress field

The nonlinear plane stress field at any material point in any component strip of the open-section thin-walled beam is obtained from the stress-strain relationship in terms of the standard ply stiffness coefficients, ($\overline{Q}$'s) which are functions of the orientation of the fibers in the ply with respect to the centroidal axis of the component strip. Expressions for the standard off-axis ply stiffness coefficients, $\overline{Q}_{ij}$, can be found, for example, in [38].

$$
\begin{aligned}
\sigma_{11} &= \epsilon_{11}[\overline{Q}_{11} + (b_{1122} + x_{n3}b_{2211})\overline{Q}_{12} + b_{1112}\overline{Q}_{16}] \\
&\quad + 2\rho_{12}[(b_{1222} + x_{n3}b_{2212})\overline{Q}_{12} + (b_{1212} + x_{n3})\overline{Q}_{16}] \\
\sigma_{22} &= \epsilon_{11}[\overline{Q}_{12} + (b_{1122} + x_{n3}b_{2211})\overline{Q}_{22} + b_{1112}\overline{Q}_{26}] \\
&\quad + 2\rho_{12}[(b_{1222} + x_{n3}b_{2212})\overline{Q}_{22} + (b_{1212} + x_{n3})\overline{Q}_{26}] \\
\sigma_{12} &= \epsilon_{11}[\overline{Q}_{16} + (b_{1122} + x_{n3}b_{2211})\overline{Q}_{26} + b_{1112}\overline{Q}_{66}] \\
&\quad + 2\rho_{12}[(b_{1222} + x_{n3}b_{2212})\overline{Q}_{26} + (b_{1212} + x_{n3})\overline{Q}_{66}] \\
\sigma_{i3} &= 0
\end{aligned} \tag{14}
$$

where the stiffness ratios $b_{\alpha\beta\gamma\delta}$ are defined as:

$$\begin{aligned}
b^n_{2212}\Delta^n &= -A^n_{22}B^n_{26}B^n_{66} + A^n_{26}({B^n_{26}}^2 + B^n_{22}B^n_{66}) \\
&\quad - {A^n_{26}}^2 D^n_{26} + A^n_{66}(A^n_{22}D^n_{26} - B^n_{22}B^n_{26}) \\
b^n_{2211}\Delta^n &= -{A^n_{26}}^2 B^n_{12} - A^n_{12}A^n_{66}B^n_{22} \\
&\quad + A^n_{26}(A^n_{16}B^n_{22} + A^n_{12}B^n_{26}) \\
&\quad + A^n_{22}(A^n_{66}B^n_{12} - A^n_{16}B^n_{26}) \\
b^n_{1112}\Delta^n &= B^n_{26}(A^n_{12}B^n_{22} - A^n_{22}B^n_{12}) \\
&\quad + A^n_{26}(B^n_{12}B^n_{22} - A^n_{12}D^n_{22}) \\
&\quad + A^n_{16}(A^n_{22}D^n_{22} - {B^n_{22}}^2) \\
b^n_{1212}\Delta^n &= B^n_{22}({B^n_{26}}^2 + A^n_{26}D^n_{26}) \\
&\quad + A^n_{22}(B^n_{66}D^n_{22} - B^n_{26}D^n_{26}) \\
&\quad - {B^n_{22}}^2 B^n_{66} - A^n_{26}B^n_{26}D^n_{22} \\
b^n_{1122}\Delta^n &= B^n_{26}(A^n_{16}B^n_{22} - A^n_{12}B^n_{26}) \\
&\quad + A^n_{66}(A^n_{12}D^n_{22} - B^n_{12}B^n_{22}) \\
&\quad + A^n_{26}(B^n_{12}B^n_{26} - A^n_{16}D^n_{22}) \\
b^n_{1222}\Delta^n &= B^n_{26}(B^n_{22}B^n_{66} + A^n_{66}D^n_{22} + A^n_{26}D^n_{26}) \\
&\quad - {B^n_{26}}^3 - A^n_{26}B^n_{66}D^n_{22} - A^n_{66}B^n_{22}D^n_{26}
\end{aligned} \tag{15}$$

The shell strain measures required to calculate the 3-D stress above are given below in terms of the 1-D strain measures:

$$\begin{aligned}
\epsilon_{11} &= \gamma_{11} + (X_{n3} + \sin\alpha_n x_{n2})\kappa_2 - (X_{n2} + \cos\alpha_n x_{n2})\kappa_3 \\
&\quad + \left[\frac{X^2_{n2} + X^2_{n3} + x^2_{n2}}{2} + x_{n2}(\cos\alpha_n X_{n2} + \sin\alpha_n X_{n3})\right](2k_1 + \kappa_1)\kappa_1 \\
&\quad + [x_{n2}(\cos\alpha_n X_{n3} - \sin\alpha_n X_{n2}) + c_n]\kappa'_1 \\
2\rho_{12} &= -2\kappa_1
\end{aligned} \tag{16}$$

3.2.3. Warping

The in-plane and out-of-plane warpings, $\overline{w}_i(x_i)$, of any material point in the n-th component strip are presented here in closed-form:

$$\begin{aligned}
\overline{w}_1 &= C_{1n} + c_n\kappa_1 + (\cos\alpha_n X_{n3} - \sin\alpha_n X_{n2})\kappa_1 x_{n2} \\
&\quad + [C_{3n} - C_{4n}(\cos\alpha_n X_{n2} + \sin\alpha_n X_{n3})](k_1 + \kappa_1)x_{n2} \\
&\quad + K^n_{11}x_{n2} + K^n_{12}x^2_{n2} + K^n_{13}x^3_{n2} + K^n_{14}x^4_{n2} + K^n_{15}x^5_{n2} \\
&\quad - x_{n3}(\cos\alpha_n X_{n2} + \sin\alpha_n X_{n3} + x_{n2})\kappa_1 \\
\overline{w}_2 &= C_{2n} + \left(K^n_{21} - \frac{C^2_{4n}}{2}\right)x_{n2} + (K^n_{22} - K^n_{32}C_{4n})x^2_{n2} \\
&\quad + (K^n_{23} - K^n_{33}C_{4n})x^3_{n2} + (K^n_{24} - K^n_{34}C_{4n})x^4_{n2} \\
&\quad + K^n_{25}x^5_{n2} + K^n_{26}x^6_{n2} + K^n_{27}x^7_{n2} \\
&\quad - x_{n3}(C_{4n} + 2K^n_{32}x_{n2} + 3K^n_{33}x^2_{n2} + 4K^n_{34}x^3_{n2}) \\
\overline{w}_3 &= C_{3n} + C_{4n}x_{n2} + K^n_{32}x^2_{n2} + K^n_{33}x^3_{n2} + K^n_{34}x^4_{n2}
\end{aligned} \tag{17}$$

where C_{1n}, C_{2n}, C_{3n} and C_{4n} are unknown coefficients. These constants represent the average first-order perturbations to the displacement measures along $\mathbf{B}_i$ and rotation about $\mathbf{B}_1$, respectively, of the n-th strip relative to the average displacements of the cross section. They can be solved for any given cross section using the continuity of displacement and rotation at all the joints and the four "rigid-body" constraints.

The coefficients K^n_{ij} are known in terms of the shell stiffness constants and 1-D strain measures as below:

$$\begin{aligned}
K^n_{32} &= -\frac{1}{2}b^n_{2211}\left[\gamma_{11} + c_n\kappa'_1 + \frac{X^2_{n2} + X^2_{n3}}{2}(2k_1\kappa_1 + \kappa_1^2) + X_{n3}\kappa_2 - X_{n2}\kappa_3\right] \\
&\quad + b^n_{2212}\kappa_1 \\
K^n_{33} &= -\frac{1}{6}b^n_{2211}[(\cos\alpha_n X_{n3} - \sin\alpha_n X_{n2})\kappa'_1 \\
&\quad + (\cos\alpha_n X_{n2} + \sin\alpha_n X_{n3})(\kappa_1^2 + 2k_1\kappa_1)] \\
&\quad - \frac{1}{6}b^n_{2211}(\sin\alpha_n\kappa_2 - \cos\alpha_n\kappa_3) \\
K^n_{34} &= -\frac{1}{24}b^n_{2211}(2k_1\kappa_1 + \kappa_1^2) \\
K^n_{11} &= b^n_{1112}\left[\gamma_{11} + c_n\kappa'_1 + \frac{X^2_{n2} + X^2_{n3}}{2}(2k_1\kappa_1 + \kappa_1^2) + X_{n3}\kappa_2 - X_{n2}\kappa_3\right] \\
&\quad - 2b^n_{1212}\kappa_1 \\
K^n_{12} &= \left[\frac{1}{2}b^n_{1112}(2k_1\kappa_1 + \kappa_1^2) - K^n_{32}(k_1 + \kappa_1)\right](\cos\alpha_n X_{n2} + \sin\alpha_n X_{n3}) \\
&\quad + \frac{1}{2}b^n_{1112}[\sin\alpha_n\kappa_2 - \cos\alpha_n\kappa_3 + (X_{n3}\cos\alpha_n - X_{n2}\sin\alpha_n)\kappa'_1] \\
K^n_{13} &= -\left[\frac{1}{3}K^n_{32} + (\cos\alpha_n X_{n2} + \sin\alpha_n X_{n3})K^n_{33}\right](k_1 + \kappa_1) \\
&\quad + \frac{1}{6}b^n_{1112}(\kappa_1^2 + 2k_1\kappa_1) \\
K^n_{14} &= -\left[\frac{1}{3}K^n_{33} + (\cos\alpha_n X_{n2} + \sin\alpha_n X_{n3})K^n_{34}\right](k_1 + \kappa_1) \\
K^n_{15} &= -\frac{3}{5}K^n_{34}(k_1 + \kappa_1) \\
K^n_{21} &= b^n_{1122}\left[\gamma_{11} + c_n\kappa'_1 + \frac{X^2_{n2} + X^2_{n3}}{2}(2k_1\kappa_1 + \kappa_1^2) + X_{n3}\kappa_2 - X_{n2}\kappa_3\right] \\
&\quad - 2b^n_{1222}\kappa_1 - \frac{1}{2}(X_{n3}\cos\alpha_n - X_{n2}\sin\alpha_n)^2\kappa_1^2 \\
K^n_{22} &= \frac{1}{2}b^n_{1122}[(\cos\alpha_n X_{n3} - \sin\alpha_n X_{n2})\kappa'_1 \\
&\quad + (\cos\alpha_n X_{n2} + \sin\alpha_n X_{n3})(\kappa_1^2 + 2k_1\kappa_1)] \\
&\quad + \frac{1}{2}b^n_{1122}(\kappa_2\sin\alpha_n - \kappa_3\cos\alpha_n) \\
K^n_{23} &= \frac{1}{6}[-4{K^n_{32}}^2 + b^n_{1122}(2k_1\kappa_1 + \kappa_1^2)] \\
K^n_{24} &= -\frac{3}{2}K^n_{32}K^n_{33} \\
K^n_{25} &= -\frac{9}{10}{K^n_{33}}^2 - \frac{8}{5}K^n_{32}K^n_{34} \\
K^n_{26} &= -2K^n_{33}K^n_{34} \\
K^n_{27} &= -\frac{8}{7}{K^n_{34}}^2
\end{aligned} \tag{18}$$

3.2.4. 1-D analysis

The nonlinear cross-sectional analysis in the previous sub-sections provide recovery relations and stiffness coefficients which are functions of the generalized 1-D strain measures. These stiffness coefficients are, in turn, needed to solve the 1-D beam problem. There are many numerical codes available to solve the 1-D beam problem. For certain specialized cases, including simple boundary conditions, closed-form solutions to the 1-D problem are possible. Solving the 1-D problem, one obtains the 1-D displacements and generalized strain measures. After both problems have been solved, the in-plane and out-of-plane warping of the cross section, the total displacement field, the 3-D strain and stress fields can all be recovered.

For a cantilever beam with restrained warping at the fixed end and either free or restrained warping at the free end, closed-form solutions are derived by solving the 1-D equilibrium equations analytically, as in Harursampath [22]. A detailed discussion on the derivation and state-of-the-art numerical solution strategies for the 1-D intrinsic equilibrium equations can be found in Hodges [26]. Restrained warping here refers to the case when warping is restricted to be zero, and free warping refers to the condition when all stresses including those due to the bi-moment are zero. Since this work is mainly concerned with the application of VAM for model reduction of a 3-D nonlinear problem to a much simpler 1-D nonlinear problem, only the final, analytical, closed-form expressions obtained for the 1-D twist, bending-rotation and axial displacements are provided here. The derivations of the same shall be dealt as a separate work. The 1-D twist, bending-rotation and axial displacements are, respectively, given by

$$\begin{aligned}
\theta_1 &= A_1\exp(\lambda x) + A_2\exp(-\lambda x) + p_1x^2 + p_2x + p_3\\
\theta_2 &= \frac{1}{2}\widetilde{g}_2x^2 + \widetilde{h}_2x - \widetilde{e}_2\theta_1\\
&\quad - \widetilde{f}_2\left[\lambda A_1\exp(\lambda x) - \lambda A_2\exp(-\lambda x) + 2p_1x + p_2\right]\\
\theta_3 &= \frac{1}{2}\widetilde{g}_3x^2 + \widetilde{h}_3x - \widetilde{e}_3\theta_1\\
&\quad - \widetilde{f}_3\left[\lambda A_1\exp(\lambda x) - \lambda A_2\exp(-\lambda x) + 2p_1x + p_2\right]\\
U_1 &= \frac{1}{2}\widetilde{g}_1x^2 + \widetilde{h}_1x - \widetilde{e}_1\theta_1\\
&\quad - \widetilde{f}_1\left[\lambda A_1\exp(\lambda x) - \lambda A_2\exp(-\lambda x) + 2p_1x + p_2\right]
\end{aligned} \tag{19}$$

where

$$\widetilde{e} = F^{-1}\begin{Bmatrix} S_{12}+S_{15}\kappa_1\\ -S_{24}-S_{45}\kappa_1\\ -S_{23}-S_{35}\kappa_1\end{Bmatrix}\quad \widetilde{f} = F^{-1}\begin{Bmatrix} S_{16}\\ -S_{46}\\ -S_{36}\end{Bmatrix}\quad \widetilde{g} = F^{-1}\begin{Bmatrix} 0\\ Q_2\\ -Q_3\end{Bmatrix} \tag{20}$$

$$\widetilde{h} = F^{-1}\begin{Bmatrix} N\\ M_2-\ell Q_2\\ M_3+\ell Q_3\end{Bmatrix}\quad F=\begin{bmatrix} S_{11} & -S_{14} & -S_{13}\\ -S_{14} & S_{44} & S_{34}\\ -S_{13} & S_{34} & S_{33}\end{bmatrix}$$

$$\lambda = \sqrt{\frac{e}{g}}\quad p_1 = -\frac{q}{2e}\quad p_2 = \frac{h}{e}\quad p_3 = -A_1 - A_2\quad A_1 = A_2 - \frac{p_2}{\lambda}$$

where, in turn,

$$\begin{aligned}
e &= S_{22} + 2S_{25}\kappa_1 + S_{55}\kappa_1^2 - \widetilde{e}_1(S_{12}+S_{15}\kappa_1)\\
&\quad + \widetilde{e}_2(S_{24}+S_{45}\kappa_1) + \widetilde{e}_3(S_{23}+S_{35}\kappa_1)\\
g &= S_{66} - \widetilde{f}_1S_{16} + \widetilde{f}_2S_{46} + \widetilde{f}_3S_{36}\\
q &= \widetilde{g}_1(S_{12}+S_{15}\kappa_1) - \widetilde{g}_2(S_{24}+S_{45}\kappa_1)\\
&\quad - \widetilde{g}_3(S_{23}+S_{35}\kappa_1)\\
h &= M_1 + \widetilde{g}_1S_{16} - \widetilde{g}_2S_{46} - \widetilde{g}_3S_{36}\\
&\quad - \widetilde{h}_1(S_{12}+S_{15}\kappa_1) + \widetilde{h}_2(S_{24}+S_{45}\kappa_1)\\
&\quad + \widetilde{h}_3(S_{23}+S_{35}\kappa_1)
\end{aligned} \tag{21}$$

In the above expressions, Q_2 and Q_3 are magnitudes of the shear forces in directions parallel to deformed basis vectors $\mathbf{B}_2$ and $\mathbf{B}_3$, respectively. Similarly N is the magnitude of the axial force which is parallel to $\mathbf{B}_1$. The expression for A_2 depends upon whether the free end of the cantilever is free to warp. For free warping,

$$A_2 = \frac{2p_1(s_1\ell + g) + p_2[s_1 - (s_1+g\ell)\exp(\lambda\ell)]}{\lambda[(s_1-g\lambda)\exp(-\lambda\ell) - (s_2+g\lambda)\exp(\lambda\ell)]} \tag{22}$$

and for restrained warping,

$$A_2 = \frac{p_2[\exp(\lambda\ell) - 1] - 2p_1\ell}{\lambda[\exp(\lambda\ell) - \exp(-\lambda\ell)]} \tag{23}$$

where

$$\begin{aligned}
s_1 &= S_{26} + S_{56}\kappa_1 - \widetilde{e}_1S_{16} + \widetilde{e}_2S_{46} + \widetilde{e}_3S_{36}\\
s_2 &= \widetilde{g}_1S_{16} - \widetilde{g}_2S_{46} - \widetilde{g}_3S_{36}\\
s_3 &= \widetilde{h}_1S_{16} - \widetilde{h}_2S_{46} - \widetilde{h}_3S_{36}
\end{aligned} \tag{24}$$

In the above equations, the rate of twist, κ_1, is an unknown and can be taken as zero initially and then iterated for. There are several measures to check the convergence of the rate of twist, κ_1, and they are as follows:

- $\kappa_1 = \frac{\theta_1}{\ell}$ can be referred as a crude but acceptable approximation.
- $\kappa_1 = \theta'_1$ provides a first approximation.
- $\kappa_1 = \theta'_1 + \frac{(\mathbf{B}_1\times\mathbf{B}'_1)\cdot\mathbf{B}'_1}{\|\mathbf{B}_1\times\mathbf{B}'_1\|^2}$ provides a better approximation, including not only the twisting curvature due to rigid-body-like rotations of the cross-sections but also torsion of the 3-D spatial curve itself.

In cases where end effects are negligible, the 1-D strain energy density of the open-section beam could alternatively be written in the following form where the stiffness matrix appears in the standard (4×4) size, which is needed as an input by many existing 1-D beam analysis codes. However, note that the elements of the second row and column below are functions of the 1-D twist rate. Hence, an iterative scheme might be needed to update the stiffness matrix input for the 1-D code.

$$U_{1D} = \frac{1}{2}\begin{Bmatrix}\gamma_{11}\\ \kappa_1\\ \kappa_2\\ \kappa_3\end{Bmatrix}^T[S_{eqv}]\begin{Bmatrix}\gamma_{11}\\ \kappa_1\\ \kappa_2\\ \kappa_3\end{Bmatrix} \tag{25}$$

where $[S_{eqv}]$ is given by

$$\begin{bmatrix} S_{11} & S_{12}+S_{15}\kappa_1 & S_{13} & S_{14}\\ S_{12}+S_{15}\kappa_1 & S_{22}+2S_{25}\kappa_1+S_{55}\kappa_1^2 & S_{23}+S_{35}\kappa_1 & S_{24}+S_{45}\kappa_1\\ S_{13} & S_{23}+S_{35}\kappa_1 & S_{33} & S_{34}\\ S_{14} & S_{24}+S_{45}\kappa_1 & S_{34} & S_{44}\end{bmatrix} \tag{26}$$

An additional two rows corresponding to transverse shear, between the existing first and second rows above, might be needed by some of the 1-D codes. As the transverse shear strains are higher order contributors to the energy for the thin-walled beams under consideration, very large artificial values for the transverse shear stiffnesses can be entered for the two additional diagonal terms in such 1-D codes. Zeroes are entered for the rest of the elements in these two rows and columns, corresponding to higher order transverse shear couplings.

It is important to note that this work provides a transition from class S to class T beams. The stiffnesses obtained for the thin-walled open-section beams are not just a trivial superimposition of the stiffnesses of the Class S beams. For example, the Vlasov effect involving κ'_1 term is not of importance asymptotically in strip-like beams (as shown by [29]) while the same is a significant term when multiple strips are put together. On the other hand, the nonlinearities associated with large flapwise bending curvatures observed in Class S beams are no longer observed in the assembly of Class S beams. These differences are an automatic fallout of the derivation rather than any additional assumptions.

4. Results and validation

The developed reduced model is implemented in MATLAB as an interactive analyzer called Open Section Beam Analyzer (OSBA) that allows for both deterministic and probabilistic solutions (through simple Monte Carlo simulations). In this part, the developed model is compared with solutions in literature for most commonly used I-section. Part II of this work deals in detail with comparison with in-house 3-D FEM solutions, comparison with FEM-based nonlinear beam models from literature and finally its applications for, both deterministic and stochastic analysis of, commonly used beam geometries.

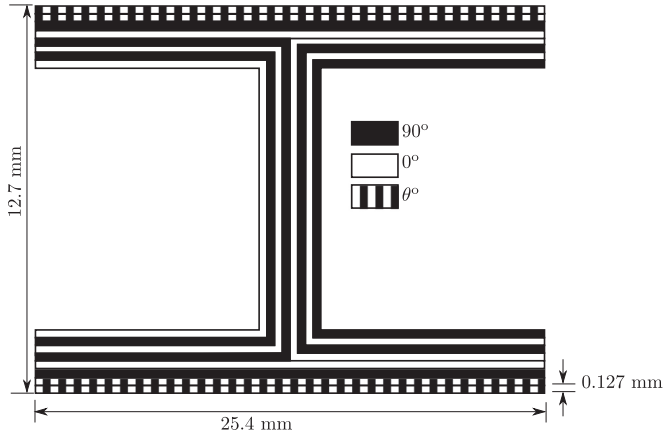

Fig. 4. Layup of I-section beam used by Chandra and Chopra [15] and used here for comparison. Two different configurations with $\theta = 15^\circ$ and $\theta = 30^\circ$ are considered.

I-section beams are among the most commonly used open-section beams and have an extensive literature available to facilitate comparisons. In this section, firstly we present the results for a general I-section behavior. The experimental work of Chandra and Chopra [15] has been used for comparison in several earlier works on I-section including Popescu and Hodges [35], Volovoi et al. [47], Badir et al. [2], Cesnik and Hodges [13], Harursampath [22]. A simplified theory, proposed by Chandra and Chopra [15], agrees well with experimental data for most of the examples considered in the work. However, due to neglect of in-plane warping, its predictive capability is shown below to be limited.

The manufacturing of I-section beams, considered here for validation, involves gluing together two channels (with four plies each) followed by the placement of remaining plies on both flanges. The I-section beam considered is as shown in Fig. 4. Hence, in order to avoid confusion, the actual layups used will be explicitly listed here. The layups used are as follows:

- Web: $[0^\circ/90^\circ/0^\circ/90^\circ/0^\circ/90^\circ/0^\circ/90^\circ]_T$
- Right side top flange: $[90^\circ/0^\circ/90^\circ/0^\circ/0^\circ/90^\circ/\theta^\circ/\theta^\circ]_T$
- Left side top flange: $[0^\circ/90^\circ/0^\circ/90^\circ/0^\circ/90^\circ/\theta^\circ/\theta^\circ]_T$
- Right side bottom flange: $[90^\circ/0^\circ/90^\circ/0^\circ/0^\circ/90^\circ/-\theta^\circ/-\theta^\circ]_T$
- Left side bottom flange: $[0^\circ/90^\circ/0^\circ/90^\circ/0^\circ/90^\circ/-\theta^\circ/-\theta^\circ]_T$.

The material properties in the original literature have been provided in Imperial units and their SI equivalents are listed here: $E_L = 141.963$ GPa, $E_T = 9.79$ GPa, $G_{LT} = 6.136$ GPa and $\nu_{LT} = 0.42$. All plies are 0.127 mm thick. The total height, width and length of the I-section beam are 12.7 mm, 25.4 mm and 762 mm respectively. Hence, the geometric parameters $\delta_h = 0.08$, $\delta_b = 0.033$ and $\delta_t = 0$ are all sufficiently small. Warping displacements are constrained at both ends and a unit tip torque (as measured in lb-in) is applied.

OSBA determines the numerical values for the cross-sectional stiffness coefficients of the I-sections under consideration using the analytical expressions derived for general open sections. The resulting stiffness matrices are presented in Tables 1 and 2 for $\theta = 15^\circ$ and $\theta = 30^\circ$ respectively. Alongside, in the tables, values obtained from OSBA are compared with results derived from the earlier works. The linear part of the present results are identical to that of Volovoi et al. [47]. The results of Badir et al. [2] would have been identical to the linearized results of the present work but for their neglect of the shell bending strain measure, ρ_{22}. The finite element analyses of Hodges and co-workers, [13,35], do not consider the thickness-to-width ratio as a small parameter and hence are more general results. However, their accuracy depends on the discretization of the cross section while the accuracy of the present results depends on how small the actual thickness-to-width ratio is when compared to unity. Chandra and Chopra [15], on the other hand, over-predict the stiffness as they assume the cross section is rigid in its own plane. The results from OSBA are also compared with the results obtained through Mathematica by Harursampath [22], and these two match exactly as shown. Using the present cross-sectional results, twist variation along the length of the cantilevered I-section beam with warping constrained at both ends (as in the experimental setup of [15]), under the application of a unit tip torque, are plotted in

Table 2
Stiffness coefficients for I-section beam ($\theta = 30^\circ$): 1-extension, 2-torsion, 3-bending, 4-bending. 5-Vlasov.

Stiffness	Present work	Volovoi et al. [47]	Badir et al. [2]	Popescu et al. [35]	Chandra et al. [15]
S_{11} (10^6 N)	4.475	4.475	4.497	4.394	5.018
S_{12} (Nm)	$161.98\kappa_1$	0	0	0	0
S_{13} (Nm)	0	0	0	0	0
S_{14} (Nm)	20.518	20.518	0	62.481	0
S_{15} (Nm^2)	0	0	0	0	0
S_{22} (Nm^2)	$0.219 + 0.009\kappa_1{}^2$	0.219	0.226	0.218	0.310
S_{23} (Nm^2)	−1.1347	−1.1347	−1.208	−1.120	−2.578
S_{24} (Nm^2)	$0.0012\kappa_1$	0	0	0	0
S_{25} (10^{-5} Nm^3)	2.624	2.624	0	0	0
S_{33} (Nm^2)	132.069	132.069	132.786	127.362	150.780
S_{34} (Nm^2)	0	0	0	0	0
S_{35} (10^{-4} Nm^3)	−7.002	−7.002	0	−4.374	0
S_{44} (Nm^2)	191.732	191.732	192.880	190.699	220.976
S_{45} (Nm^3)	0	0	0	0	0
S_{55} (10^{-3} Nm^4)	6.543	6.543	6.582	7.419	7.550

Table 1
Stiffness coefficients for I-section beam ($\theta = 15^\circ$): 1-extension, 2-torsion, 3-bending, 4-bending, 5-Vlasov.

Stiffness	Present work	Volovoi et al. [47]	Badir et al. [2]	Popescu et al. [35]	Cesnik et al. [13]	Chandra et al. [15]
S_{11} (10^6 N)	5.133	5.133	5.142	5.049	5.049	5.525
S_{12} (Nm)	$190.92\kappa_1$	0	0	0	0	0
S_{13} (Nm)	0	0	0	0	0	0
S_{14} (Nm)	15.072	15.072	0	57.735	34.2683	0
S_{15} (Nm^2)	0	0	0	0	NA	0
S_{22} (Nm^2)	$0.178 + 0.0165\kappa_1$	0.178	0.178	0.178	0.178	0.193
S_{23} (Nm^2)	−1.278	−1.278	−1.295	−1.352	−1.349	−1.827
S_{24} (10^{-4} Nm^2)	$8.65\kappa_1$	0	0	0	0	0
S_{25} (10^{-5} Nm^3)	1.145	1.145	0	0	NA	0
S_{33} (Nm^2)	154.54	154.54	154.855	152.789	152.703	153.937
S_{34} (Nm^2)	0	0	0	0	0	0
S_{35} (10^{-4} Nm^3)	−5.144	−5.144	0	−4.374	NA	0
S_{44} (Nm^2)	227.146	227.146	227.662	225.682	225.539	248.526
S_{45} (Nm^3)	0	0	0	0	NA	0
S_{55}(10^{-3} Nm^4)	7.752	7.752	7.771	8.154	NA	8.491

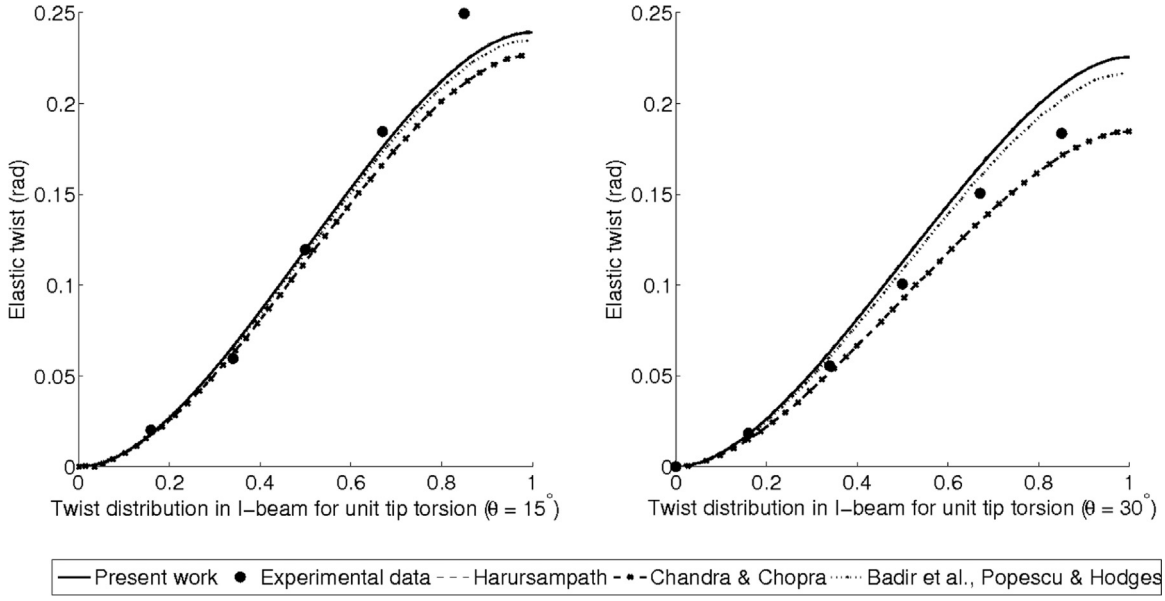

Fig. 5. Twist distribution along the length of I-section beam for unit tip torque: ($\theta = 15°$) (Left); ($\theta = 30°$) (Right).

Fig. 5. Comparisons with previous results are also shown. The present results show better correlation with experiments than the previous results for the case of $\theta = 15°$. At the tip of the cantilever, all the theories presented or compared here exhibit relatively larger deviations from the experiments probably because of the idealization of constrained warping at the tip. In reality, the situation might be somewhere in-between that of constrained warping and free warping at the tip. Additionally, it is important to note that the works of Cesnik and Hodges [13]; Badir et al. [2] have also been directly used for the validation of VABS in the work of Yu et al. [55]. Thus, this comparison provides an indirect comparison with the results of VABS too.

5. Conclusions and future work

The theory presented in this work is part of an overall framework of tools under development for cross-sectional analysis of rotor blades and other slender, anisotropic structural members. The overall goals include development of finite element approaches for reduced arbitrary, built-up cross-sectional geometries and closed-form expressions for thin-walled cross sections with arbitrary geometry.

This work while targeting the nonlinear strain field phenomena in thin-walled composite beams has resulted in the development of a unified theory in closed-form incorporating all the non-classical effects which contribute to the energy terms of the same order as the classical terms, due to the presence of small geometric parameters in the structures. Few approaches are available in the literature to analyze the nonlinear “trapeze effect” for anisotropic beams of arbitrary geometry. Since they are not based on asymptotic approaches, the asymptotical correctness of these analyses is difficult to assess.

To conclude, this work shows that the non-classical nonlinearities being brought into prominence in open-section beams are due to the thin walls which undergo large warping due to elastic twist. In general, this could be excited in any beam, because generally anisotropic materials are considered here. Thus, this work demonstrates a class transition from Class S to Class T beams by capturing the relevant non-classical nonlinearities analytically, and in an asymptotically-correct manner, for specific geometries.

In addition, most of the FEM-based solutions use beam and shell based models rather than full 3-D FEM solutions. The nonlinearity arising due to the anisotropy in the material further render full 3-D FEM solutions computationally intensive. There are no known full 3-D FEM solutions, in literature, for the T-class composite beams presented here.

Some works like Blasques et al. [8] demonstrate 3-D FEM solutions for R-class beams. However, R-class beams do not demonstrate the nonlinear and non-classical effects that are observed in S- and T-class beams as discussed in this work.

Part II demonstrates application of the developed theory is applied to open-sections beams of commonly used cross-section (I-, Z-, T-, star-sections). The solutions are compared with results available in literature based on nonlinear beam elements developed in FEM and also in-house full 3-D FEM solutions generated using Abaqus. Detailed discussions are provided regarding the implications of the developed theory. Finally, the computational efficiency of the developed model is demonstrated by application to stochastic analysis where uncertainties in material and geometric properties are considered to analyze up to five million samples in a matter of minutes.

References

[1] E.A. Armanios, A. Makeev, D. Hooke, Finite displacement analysis of laminated composite strips with extension-twist coupling, J. Aerosp. Eng. 9 (3) (1996) 80–91.
[2] A.M. Badir, V.L. Berdichevsky, E.A. Armanios, Theory of composite thin-walled open cross section beams, in: Proceedings of the 34th AIAA Structures, Structural Dynamics and Materials Conference, La Jolla, California, 1993, pp. 2761–2770.
[3] V.L. Berdichevsky, Variational-asymptotic method of shell theory construction, J. Appl. Math. Mech. 43 (4) (1979) 664–687.
[4] V.L. Berdichevsky, On the energy of an elastic rod, J. Appl. Math. Mech. 45 (1982) 518–529.
[5] V.L. Berdichevsky, E.A. Armanios, A.M. Badir, Theory of anisotropic thin-walled closed-section beams, Compos. Eng. 2 (5–7) (1992) 411–432.
[6] V.L. Berdichevsky, L.A. Starosel'skii, On the theory of curvilinear Timoshenko-type rods, J. Appl. Math. Mech. 47 (6) (1983) 809–817.
[7] M.A. Biot, Increase of torsional stiffness of a prismatical bar due to axial tension, J. Appl. Phys. 10 (1939) 860–864.
[8] J.P. Blasques, R.D. Bitsche, V. Fedorov, B.S. Lazarov, Accuracy of an efficient framework for structural analysis of wind turbine blades, Wind Energy 19 (2016) 1603–1621.
[9] M. Borri, T. Merlini, A large displacement formulation for anisotropic beam analysis, Meccanica 21 (1986) 30–37.
[10] J.C. Buckley, The bifilar property of twisted strips, Philos. Mag. 28 (1914) 778–785.
[11] C.E.S. Cesnik, D.H. Hodges, Stiffness constants for initially twisted and curved composite beams, Appl. Mech. Rev. 46 (11(2)) (1993) S211–S220.
[12] C.E.S. Cesnik, D.H. Hodges, Stiffness constants for composite beams including large initial twist and curvature effects, Appl. Mech. Rev. 48 (11(2)) (1995) S61–S67.
[13] C.E.S. Cesnik, D.H. Hodges, VABS: a new concept for composite rotor blade cross-sectional modeling, J. Am. Helicopter Soc. 42 (1) (1997) 27–38.
[14] C.E.S. Cesnik, D.H. Hodges, V.G. Sutyrin, Cross-sectional analysis of composite beams including large initial twist and curvature effects, AIAA J. 34 (9) (1996) 1913–1920.

[15] R. Chandra, I. Chopra, Experimental and theoretical analysis of composite I-beams with elastic coupling, AIAA J. 29 (12) (1991) 2197–2206.
[16] D.A. Danielson, D.H. Hodges, Nonlinear beam kinematics by decomposition of rotation tensor, J. Appl. Mech. 54 (2) (1987) 258–262.
[17] S. Gabriele, N. Rizzi, V. Varano, A 1d nonlinear twb model accounting for in plane cross-section deformation, Int. J. Solids Struct. 94–95 (2016) 170–178.
[18] G. Garcea, R. Goncalves, A. Bilotta, D. Manta, R. Bebiano, L. Leonetti, D. Magisano, D. Camotim, Deformation modes of thin-walled members: a comparison between the method of generalized eigenvectors and generalized beam theory, Thin Walled Struct., 100, 2016, pp. 192–212.
[19] A. Genoese, A. Genoese, A. Bilotta, G. Garcea, Buckling analysis through a generalized beam model including section distortions, Thin Walled Struct. 85 (2014) 125–141.
[20] A. Genoese, A. Genoese, A. Bilotta, G. Garcea, A generalized model for heterogeneous and anisotropic beams including section distortions, Thin Walled Struct. 74 (2014) 85–103.
[21] J.N. Goodier, Elastic torsion in the presence of initial axial stress, in: Proceedings of the ASME Annual Conference of the Applied Mechanics Division, Purdue University, Lafayette, Ind, 1950.
[22] D. Harursampath, Non-classical non-linear effects in thin walled composite beams, (Ph.D. thesis), Georgia Institute of Technology, Daniel Guggenheim School of Aerospace Engineering, Atlanta, GA, USA, 1998.
[23] D. Harursampath, D.H. Hodges, Asymptotic analysis of non-linear behavior of long anisotropic tubes, Int. J. Non-Linear Mech. 34 (6) (1999) 1003–1018.
[24] D.H. Hodges, Torsion of pretwisted beams due to axial loading, J. Appl. Mech. 47 (1980) 393–397.
[25] D.H. Hodges, Geometrically-exact, intrinsic theory for dynamics of curved and twisted anisotropic beams, AIAA J. 41 (6) (2003) 1131–1137.
[26] D.H. Hodges, Nonlinear Composite Beam Theory, American Institute of Aeronautics and Astronautics, 2006.
[27] D.H. Hodges, A.R. Atilgan, C.E.S. Cesnik, M.V. Fulton, On a simplified strain energy function for geometrically nonlinear behavior of anisotropic beams, Compos. Eng. 2 (5–7) (1992) 513–526.
[28] D.H. Hodges, E.H. Dowell, Nonlinear equations of motion for the elastic bending and torsion of twisted nonuniform rotor blades, Tech. Rep. TN D-7818, NASA, 1974.
[29] D.H. Hodges, D. Harursampath, V.V. Volovoi, C.E.S. Cesnik, Non-classical effects in non-linear analysis of anisotropic strips, Int. J. Non-Linear Mech. 34 (2) (1999) 259–277.
[30] J.C. Houbolt, G.W. Brooks, Differential equations of motion for combined flapwise bending, chordwise bending and torsion of twisted nonuniform rotor blades, Tech. Rep. 1346, NACA, 1957.
[31] T.-T. Nguyen, P.T. Thang, J. Lee, Flexural-torsional stability of thin-walled functionally graded open-section beams, Thin Walled Struct. 110 (2017) 88–96.
[32] R. Palacios, C.E.S. Cesnik, Cross-sectional analysis of nonhomogeneous anisotropic active slender structures, AIAA J. 43 (12) (2005) 2624–2638.
[33] R. Palacios, C.E.S. Cesnik, Geometrically nonlinear theory of composite beams with deformable cross-sections, AIAA J. 46 (2) (2008) 439–450.
[34] B. Popescu, Asymptotically correct refinements in numerical cross-sectional analysis of composite beams, (Ph.D. thesis), Georgia Institute of Technology, Atlanta, Georgia, U.S.A, 1998.
[35] B. Popescu, D.H. Hodges, Asymptotic treatment of the trapeze effect in finite element cross-sectional analysis of composite beams, Int. J. Non-Linear Mech. 34 (1999) 709–721.
[36] B. Popescu, D.H. Hodges, On asymptotically correct Timoshenko-like anisotropic beam theory, Int. J. Solids Struct. 37 (3) (2000) 535–558.
[37] B. Popescu, D.H. Hodges, C.E.S. Cesnik, Obliqueness effects in asymptotic cross-sectional analysis of composite beams, Comput. Struct. 76 (4) (2000) 533–543.
[38] J.N. Reddy, Mechanics of Laminated Composite Plates and Shells: Theory and Analysis, CRC Press, 2004.
[39] E. Reissner, On one-dimensional large-displacement finite-strain beam theory, Stud. Appl. Math. LII 2 (1973) 87–95.
[40] A. Rosen, The effect of initial twist on the torsional rigidity of beams - another point of view, J. Appl. Mech. 47 (1980) 389–392.
[41] S. Roy, W. Yu, An asymptotically correct model for initially curved and twisted thin-walled composite beams, Int. J. Solids Struct. 44 (11–12) (2007) 4039–4052.
[42] Z. Sotoudeh, D.H. Hodges, Modeling beams with various boundary conditions using fully intrinsic equations, J. Appl. Mech. 78 (3) (2011) 031010.
[43] V.V. Volovoi, On end effects in prismatic beams, (Ph.D. thesis), Georgia Institute of Technology, Atlanta, Georgia, U.S.A, 1997.
[44] V.V. Volovoi, D.H. Hodges, Theory of anisotropic thin-walled beams, J. Appl. Mech. 67 (3) (2000) 453–459.
[45] V.V. Volovoi, D.H. Hodges, Single- and multi-celled composite thin-walled beams, AIAA J. 40 (5) (2002) 960–965.
[46] V.V. Volovoi, D.H. Hodges, V.L. Berdichevsky, Asymptotic theory for static behavior of elastic anisotropic I-beams, Int. J. Solids Struct. 36 (7) (1999) 1017–1043.
[47] V.V. Volovoi, D.H. Hodges, V.L. Berdichevsky, V.G. Sutyrin, Asymptotic theory of static behavior of elastic anisotropic I-beams, Int. J. Solids Struct. 36 (7) (1999) 1017–1043.
[48] H. Wagner, Torsion and buckling of open-sections, Tech. Rep. TM 807, NASA, 1936.
[49] W. Yu, D.H. Hodges, An asymptotic approach for thermoelastic analysis of laminated composite plates, J. Eng. Mech. 130 (5) (2004) 531–540.
[50] W. Yu, D.H. Hodges, Elasticity solutions versus asymptotic sectional analysis of homogeneous, isotropic, prismatic beams, J. Appl. Mech. 71 (1) (2004) 15–23.
[51] W. Yu, D.H. Hodges, J.C. Ho, Variational asymptotic beam sectional analysis – an updated version, Int. J. Eng. Sci. 59 (2012) 40–64.
[52] W. Yu, D.H. Hodges, V.V. Volovoi, C.E.S. Cesnik, On Timoshenko-like modeling of initially curved and twisted composite beams, Int. J. Solids Struct. 39 (19) (2002) 5101–5121.
[53] W. Yu, D.H. Hodges, V.V. Volovoi, E.D. Fuchs, A generalized Vlasov theory for composite beams, Thin-Walled Struct. 43 (9) (2005) 1493–1511.
[54] W. Yu, L. Liao, D.H. Hodges, V.V. Volovoi, Theory of initially twisted, composite, thin-walled beams, Thin Walled Struct. 43 (8) (2005) 1296–1311.
[55] W. Yu, V.V. Volovoi, D.H. Hodges, X. Hong, Validation of variational asymptotic beam sectional (VABS) analysis, AIAA J. 40 (10) (2002) 2105–2112.